

Next-To-Leading-Order Matching for the Magnetic Photon-Penguin Operator in the $B \rightarrow X_s \gamma$ Decay

Andrzej J. Buras, Axel Kwiatkowski and Nicolas Pott

*Technische Universität München, Physik Department
D-85748 Garching, Germany*

Abstract

The initial condition at the matching scale $\mu_W = \mathcal{O}(M_W)$ for the Wilson coefficient of the magnetic photon-penguin operator in the decay $B \rightarrow X_s \gamma$ is calculated in the next-to-leading-order approximation. The technical details of the necessary two-loop calculation in the full theory are described and the matching with the corresponding result in the effective theory is discussed in detail. Our outcome for the initial condition confirms the final results of Adel and Yao and Greub and Hurth. We show that — contrary to the claims in the second of these papers — the matching procedure can be properly performed for infrared divergent amplitudes, i. e. independently of contributions from gluon bremsstrahlung.

Supported by the German Bundesministerium für Bildung and Forschung under contract 06 TM 874
and DFG Project Li 519/2-2.

1 Introduction

The inclusive rare B meson decay $B \rightarrow X_s \gamma$ plays an important role in present day phenomenology. In the Standard Model it originates at the one-loop level in the so-called magnetic penguin diagrams and receives considerable QCD corrections [1]. Since it is a loop-induced decay, it is naturally suppressed and simultaneously sensitive to physics beyond the Standard Model. However, in order to discover some new physics in $B \rightarrow X_s \gamma$ it is essential that both the experimental data and the theoretical prediction in the Standard Model for this decay reach sufficient precision.

Experimentally, the branching ratio for $B \rightarrow X_s \gamma$ is found by the CLEO collaboration to be [2]

$$\mathcal{B}[B \rightarrow X_s \gamma] = (2.32 \pm 0.57 \pm 0.35) \times 10^{-4}, \quad (1)$$

and a very preliminary result from the ALEPH collaboration reads [3]

$$\mathcal{B}[B \rightarrow X_s \gamma] = (3.38 \pm 0.74 \pm 0.85) \times 10^{-4}. \quad (2)$$

In (1) and (2) the first error is statistical and the second is systematic. While these results put already some constraints on the physics beyond the Standard Model, the experimental errors have to be considerably reduced before some firm conclusions can be reached.

On the theoretical side, during the last five years a considerable effort has been made to calculate the important QCD effects in this decay, including next-to-leading-order (NLO) corrections in renormalization group improved perturbation theory. One of the main motivations for this enterprise were $\pm 25\%$ renormalization scale uncertainties [4,5] in the leading order branching ratio which — as anticipated in [5] — could only be reduced by extending the calculations beyond the leading order.

Fortunately as of 1997 the complete NLO corrections to the $B \rightarrow X_s \gamma$ decay are known. It was a joint effort of many groups. The $\mathcal{O}(\alpha_s)$ corrections to the initial conditions for the Wilson coefficients of the relevant magnetic penguin operators at the scale $\mu_W = \mathcal{O}(M_W)$ have been calculated in [6] and confirmed in [7]. The next-to-leading 8×8 anomalous dimension matrix necessary for the renormalization group evolution of the Wilson coefficients from $\mu = \mu_W = \mathcal{O}(M_W)$ down to $\mu = \mu_b = \mathcal{O}(m_b)$ has been calculated in [8–13] of which [8–12] are two-loop calculations and [13] is a very difficult three-loop calculation. The one-loop matrix elements $\langle s\gamma|Q_i|b \rangle$ and the gluon bremsstrahlung contributions $\langle s\gamma g|Q_i|b \rangle$ have been calculated in [14,15]. Finally, the very difficult two-loop corrections to $\langle s\gamma|Q_i|b \rangle$ were presented in [16].

In a recent letter [17] we have analyzed the scale uncertainties in the $B \rightarrow X_s \gamma$ decay including not only the scale uncertainty in μ_b considered in the papers above, but also the uncertainties in

the choice of μ_W and the choice of the scale μ_t entering the running top quark mass $\overline{m}_t(\mu_t)$. To this end we have repeated the calculation of the initial condition of the by far dominant Wilson coefficient of the magnetic photon-penguin operator Q_7 confirming the final result in [6, 7] and generalizing it to include the dependences on μ_t and μ_W with $\mu_t \neq \mu_W$. In [6] and [7] $\mu_W = \mu_t$ was used. Our numerical analysis of the complete NLO corrections gave

$$\mathcal{B}[B \rightarrow X_s \gamma] = (3.48 \pm 0.13(\text{scale}) \pm 0.28(\text{par})) \times 10^{-4} = (3.48 \pm 0.31) \times 10^{-4} \quad (3)$$

where we show separately scale and parametric uncertainties.

The new feature of this result compared to the previous NLO analyses [13, 16] is the smallness of the remaining scale uncertainties by a factor of two relative to the ones quoted in these papers. The origin of this difference, which is related to the numerical analysis, has been discussed in detail in [17] and will not be repeated here. This welcome reduction of the scale uncertainties cannot be fully appreciated at present because of considerable parametric uncertainties originating dominantly in the charm and bottom quark masses. We believe that these parametric uncertainties will be reduced in the future by at least a factor of two, so that a prediction for $\mathcal{B}[B \rightarrow X_s \gamma]$ with an uncertainty of 5 – 10% will be available one day. With more precise measurements of $\mathcal{B}[B \rightarrow X_s \gamma]$ expected from the upgraded CLEO detector as well as from the B factories at SLAC and KEK this should allow a useful test of the Standard Model, possibly giving some hints beyond it.

The purpose of the present paper is the presentation of the details of our calculation of the initial condition for the Wilson coefficient $C_7(\mu_W)$ of the magnetic photon-penguin operator. This initial condition is obtained from a matching of the full theory (involving the W boson and the top quark) with the effective theory in which W and top do not appear as dynamical degrees of freedom: they have been integrated out.

Since our result agrees with the previous calculations done in [6] and [7] we would like to point out right away what is new in our paper.

Our method is very similar to the one used by Greub and Hurth [7] and will be explained in the following sections. In [7] dimensional regularization ($D = 4 - 2\varepsilon$) is used to regulate both infrared and ultraviolet singularities. It has been stressed there that in order to obtain the final result for $C_7(\mu_W)$ it is essential

1. to distinguish the $1/\varepsilon$ ultraviolet singularities from the infrared ones, which in [7] are denoted by $1/\varepsilon_{\text{IR}}$,
2. that the matching between the full and the effective theory is done in $D = 4$ dimensions and that it can only be performed for infrared finite quantities. In our case this would mean that also the contributions from bremsstrahlung ($b \rightarrow s \gamma g$) have to be considered.

We disagree on both points. First of all it is certainly not necessary to use different ε 's for ultraviolet and infrared divergences which simplifies considerably the calculations and avoids the appearance of dubious terms like $\varepsilon/\varepsilon_{\text{IR}}$ in [7]. After proper renormalization of ultraviolet singularities the left-over divergences are of infrared origin only. These singularities will automatically cancel in the matching procedure since the Wilson coefficients are purely short-distance quantities, independent of the infrared structure of the theory. This implies contrary to Greub and Hurth that the matching of the full and the effective theory can correctly be done for infrared divergent quantities. In particular, as we will demonstrate in this paper, it can be performed by considering only the virtual corrections to the decay $b \rightarrow s\gamma$, i. e. without invoking the process $b \rightarrow s\gamma g$. To this end, however, it is essential to perform the matching in $D = 4 - 2\varepsilon$ dimensions. This requires that $\mathcal{O}(\varepsilon)$ terms in the Wilson coefficients have to be kept during the calculation until all infrared divergences present in the full theory have been cancelled in the process of matching by those present in the effective theory. The authors of [7] did not keep these $\mathcal{O}(\varepsilon)$ terms which is correct if one restricts oneself to infrared finite quantities. However, this restriction implies that — at least in principle — the matching has to be done on the level of the decay rate (i. e. including bremsstrahlung), whereas in our approach the matching can be performed in a straight forward manner between amplitudes. We regard this as a conceptual advantage. Despite of this Greub and Hurth formulated the matching condition in their work for infrared finite amplitudes which they constructed by subtraction of pure $1/\varepsilon_{\text{IR}}$ poles as well as $\varepsilon/\varepsilon_{\text{IR}}$ terms. However, they do not show explicitly that bremsstrahlung contributions can justify this definition.

To demonstrate our points, we think it is useful and profitable for future calculations of this sort to provide an explicit presentation of our NLO calculation of $C_7(\mu_W)$.

Our paper is organized as follows: In Section 2 we recall briefly the theoretical framework for the $B \rightarrow X_s\gamma$ decay. In Section 3 we outline the matching procedure and discuss the issue of the $\mathcal{O}(\varepsilon)$ -terms in the Wilson coefficients in explicit terms. In Section 4 the calculations in the full theory are presented. Here we also review briefly the Heavy Mass Expansion method. In Section 5 the corresponding calculations in the effective theory are described. The final result for $C_7^{(1)}(\mu_W)$ is given in Section 6. Section 7 briefly summarizes our paper.

2 Theoretical Framework

Perturbative QCD effects to the theoretical prediction for the $B \rightarrow X_s\gamma$ decay are associated with large logarithms $\alpha_s^n(\mu_b) \ln^m(\mu_W/\mu_b)$ ($m \leq n$), where μ_W is a scale of the order of M_W or m_t and $\mu_b \simeq m_b$ is the scale of the hadronic decay under consideration. The resummation of

these logarithms to all orders in leading ($n = m$) or next-to-leading ($n = m + 1$) approximation is achieved in the framework of a low energy theory where all heavy particles like the W boson and the top quark are integrated out. The effective Hamiltonian relevant for $B \rightarrow X_s \gamma$ reads

$$\mathcal{H}^{\text{eff}} = -\frac{G_F}{\sqrt{2}} \lambda_t \sum_{i=1}^8 C_i(\mu) Q_i \equiv -\frac{G_F}{\sqrt{2}} \lambda_t \vec{Q}^T \vec{C}(\mu) \quad (4)$$

with the CKM factor $\lambda_q = V_{qb} V_{qs}^*$. The current-current operators Q_1, Q_2 and the QCD penguin operators Q_3, \dots, Q_6 can be found e.g. in Eq. (IX.2) of [18]. Here we only list the magnetic photon-penguin and the magnetic gluon-penguin operators

$$Q_7 = \frac{e}{8\pi^2} m_b \bar{s}_\alpha \sigma^{\mu\nu} (1 + \gamma_5) b_\alpha F_{\mu\nu}, \quad Q_8 = \frac{g_s}{8\pi^2} m_b \bar{s}_\alpha \sigma^{\mu\nu} (1 + \gamma_5) T_{\alpha\beta}^a b_\beta G_{\mu\nu}^a \quad (5)$$

where the contributions from the mass insertions on the external s -quark line are neglected due to the approximation $m_s \ll m_b$.

Although matrix elements $\langle \mathcal{H}^{\text{eff}} \rangle$ of the effective Hamiltonian (4) are physical and therefore renormalization scale invariant quantities, the separate μ -dependence of the Wilson coefficients $C_i(\mu)$ and the matrix elements $\langle Q_i(\mu) \rangle$ reflects the factorization of short-distance and long-distance physics. The scale dependence of the coefficient functions is governed by the renormalization group equation

$$\mu \frac{d}{d\mu} \vec{C}(\mu) = \hat{\gamma}^T(\alpha_s) \vec{C}(\mu) \quad (6)$$

where $\hat{\gamma}(\alpha_s)$ is the 8×8 anomalous dimension matrix. The solution of (6) is given by

$$\vec{C}(\mu_b) = \hat{U}(\mu_b, \mu_W) \vec{C}(\mu_W) \quad (7)$$

where $\hat{U}(\mu_b, \mu_W)$ is an evolution matrix from μ_W down to μ_b and $\vec{C}(\mu_W)$ are the initial conditions for this evolution. An explicit formula for \hat{U} in terms of $\hat{\gamma}(\alpha_s)$ is given e.g. in Eq. (III.93) of [18]. The initial conditions $\vec{C}(\mu_W)$ for the operators Q_1, Q_2 and Q_3, \dots, Q_6 , calculated in [9] and [10] respectively, can also be found there. The purpose of the present paper is the calculation of $\mathcal{O}(\alpha_s)$ corrections to $C_7(\mu_W)$.

3 Outline of the Matching Procedure

Since the Wilson coefficients are independent of the external states in the matrix elements, the initial conditions may be determined by considering the decay process at the quark level $b \rightarrow s \gamma$. They are obtained by matching the full and the effective theory at the matching scale $\mu = \mu_W$. Therefore the matrix element $\mathcal{M}(b \rightarrow s \gamma)$ is first to be calculated in the full theory which contains the full particle spectrum of the Standard Model. At the NLO level this amounts to

the computation of two-loop diagrams as depicted in Figure 1, where heavy particles like the top quark, W^\pm bosons and Higgs-ghosts Φ^\pm explicitly appear as virtual states. The result has the following structure:

$$\mathcal{M}(b \rightarrow s\gamma) = -\frac{G_F}{\sqrt{2}} \lambda_t K_7(\mu) \langle s\gamma | Q_7 | b \rangle^{(0)} \equiv \mathcal{M}^{(0)} + \mathcal{M}^{(1)} \quad (8)$$

where the respective terms $\mathcal{M}^{(0)}$ and $\mathcal{M}^{(1)}$ of the zeroth and first order in α_s correspond to the decomposition of K_7

$$K_7(\mu) = K_7^{(0)}(\mu) + \frac{\alpha_s}{4\pi} K_7^{(1)}(\mu). \quad (9)$$

Furthermore, $\langle s\gamma | Q_7 | b \rangle^{(0)}$ denotes the tree level matrix element of Q_7 .

In a second step the calculation of the matrix element in the effective theory $\hat{\mathcal{M}}(b \rightarrow s\gamma)$ is required, where all heavy particles have been integrated out. Accordingly the diagrams in Figure 2 are composed of light particles only. Using the shorthand notation $\langle Q_i \rangle \equiv \langle s\gamma | Q_i | b \rangle$ and the expansions

$$C_i(\mu) = C_i^{(0)}(\mu) + \frac{\alpha_s}{4\pi} C_i^{(1)}(\mu), \quad \langle Q_i(\mu) \rangle = \langle Q_i \rangle^{(0)} + \frac{\alpha_s}{4\pi} \langle Q_i(\mu) \rangle^{(1)}, \quad (10)$$

the matrix element in the effective theory is written as

$$\begin{aligned} \hat{\mathcal{M}}(b \rightarrow s\gamma) &= \sum_{i=1}^8 \hat{\mathcal{M}}_i = -\frac{G_F}{\sqrt{2}} \lambda_t \sum_{i=1}^8 C_i(\mu) \langle Q_i(\mu) \rangle \\ &= -\frac{G_F}{\sqrt{2}} \lambda_t \sum_{i=1}^8 \left(C_i^{(0)}(\mu) \langle Q_i \rangle^{(0)} + \frac{\alpha_s}{4\pi} [C_i^{(0)}(\mu) \langle Q_i(\mu) \rangle^{(1)} + C_i^{(1)}(\mu) \langle Q_i \rangle^{(0)}] \right). \end{aligned} \quad (11)$$

The matching procedure between the full and the effective theory establishes the initial conditions for the Wilson coefficients. The matching scale μ_W is chosen in the regime $\mu_W \simeq \mathcal{O}(M_W, m_t)$, thus giving rise only to small logarithms $\alpha_s \ln(\mu_W/M_W)$ in the perturbative expansion. The matching condition

$$\hat{\mathcal{M}}(\mu_W) = \mathcal{M}(\mu_W) \quad (12)$$

translates into the LO and NLO identities

$$\text{LO : } C_7^{(0)}(\mu_W) = K_7^{(0)}(\mu_W), \quad (13)$$

$$\text{NLO : } \sum_{i=1}^8 \left(C_i^{(0)}(\mu_W) \langle Q_i(\mu_W) \rangle^{(1)} + C_i^{(1)}(\mu_W) \langle Q_i \rangle^{(0)} \right) = K_7^{(1)}(\mu_W) \langle Q_7 \rangle^{(0)}. \quad (14)$$

Anticipating the results for the various coefficients that will explicitly be presented below, we would like to stress once more our treatment of infrared singularities in the problem. In contrast to the authors of [7], we have not distinguished between infrared ($1/\varepsilon_{\text{IR}}$) and ultraviolet

($1/\varepsilon_{\text{UV}}$) poles in our calculation. Although our IR and UV singularities are also dimensionally regularized, a distinction between ε_{IR} and ε_{UV} becomes irrelevant, once ε is analytically continued from the region of convergent integrals to arbitrary values. Nevertheless, at the end of the two-loop calculation of $K_7^{(1)}$ one ends up with remaining pole terms even after the UV renormalization has been performed. These pole terms are easily identified as IR divergences on physical grounds. Similar pole terms occur in the effective theory during the calculation of the one-loop corrections to the operator matrix elements $\langle s\gamma|Q_7|b\rangle^{(1)}$ and $\langle s\gamma|Q_8|b\rangle^{(1)}$. These IR singularities cancel out in the matching procedure due to a compensation between the full and the effective theory.

From the NLO matching relation (14) one observes that the $\mathcal{O}(\varepsilon)$ terms in $C_i^{(0)}$ yield a finite contribution when being combined with the singular piece of $\langle s\gamma|Q_i|b\rangle^{(1)}$. The initial condition $C_7^{(1)}(\mu_W)$ is therefore obtained from the NLO relation (14), but it requires the LO matching to be performed up to $\mathcal{O}(\varepsilon)$ in (13) as emphasized already in Section 1. Decomposing the leading order Wilson coefficients accordingly,

$$C_i^{(0)} = C_{i0}^{(0)} + \varepsilon C_{i\varepsilon}^{(0)}, \quad (15)$$

the results for $C_7^{(0)}$ and $C_8^{(0)}$ obtained from the matching relation (13) read

$$C_{70}^{(0)}(\mu_W) = \frac{3x_t^3 - 2x_t^2}{4(x_t - 1)^4} \ln x_t + \frac{-8x_t^3 - 5x_t^2 + 7x_t}{24(x_t - 1)^3}, \quad (16)$$

$$C_{80}^{(0)}(\mu_W) = \frac{-3x_t^2}{4(x_t - 1)^4} \ln x_t + \frac{-x_t^3 + 5x_t^2 + 2x_t}{8(x_t - 1)^3} \quad (17)$$

and for the ε -terms

$$\begin{aligned} C_{7\varepsilon}^{(0)}(\mu_W) = & C_{70}^{(0)} \ln \frac{\mu_W^2}{M_W^2} + \frac{7x_t(1+x_t)(5-8x_t)}{144(x_t-1)^3} \\ & + \frac{x_t(48-162x_t+157x_t^2-22x_t^3)}{72(x_t-1)^4} \ln x_t + \frac{x_t^2(2-3x_t)}{8(x_t-1)^4} \ln^2 x_t, \end{aligned} \quad (18)$$

$$\begin{aligned} C_{8\varepsilon}^{(0)}(\mu_W) = & C_{80}^{(0)} \ln \frac{\mu_W^2}{M_W^2} - \frac{x_t(26-93x_t+25x_t^2)}{48(x_t-1)^3} \\ & + \frac{x_t(24-54x_t+14x_t^2-5x_t^3)}{24(x_t-1)^4} \ln x_t + \frac{3}{8} \frac{x_t^2}{(x_t-1)^4} \ln^2 x_t \end{aligned} \quad (19)$$

respectively. Here the notation

$$x_t = \frac{\overline{m}_t^2(\mu_t^2)}{M_W^2} \quad (20)$$

is used where μ_t is the scale chosen to define the running top quark mass.

The results (16)–(19) are obtained by calculating the usual one-loop magnetic penguin diagrams including $\mathcal{O}(\varepsilon)$ terms. The results in (16) and (17) are the well known leading order initial

conditions for the operators Q_7 and Q_8 respectively. The results given in (18) and (19) agree with the corresponding expressions in [7] where they have been denoted by K_{701} and K_{801} respectively. The authors of [7] kept these $\mathcal{O}(\varepsilon)$ terms only in calculating the renormalization counterterms in the full theory. As we stressed in Section 1, in our approach they have to be kept in the effective theory as well.

4 Calculation of $b \rightarrow s\gamma$ in the Full Theory

4.1 Preliminary Remarks

For the calculation of the matrix element $\mathcal{M}(b \rightarrow s\gamma)$ in the full theory the two-loop diagrams of Figure 1 have to be considered. They are grouped into four different classes according to a corresponding classification of integrals. Topologically the diagrams come in two copies of the same set, because the virtually exchanged quark may be the top or the charm quark. We neglect the third possibility of an internal up quark due to the smallness of $\lambda_u = V_{ub}V_{us}^* \approx 0$. As a consequence the unitarity relation $\lambda_t + \lambda_c + \lambda_u = 0$ becomes

$$\lambda_c = -\lambda_t. \quad (21)$$

This justifies the overall CKM factor λ_t in (4). Working in the 't Hooft-Feynman gauge the virtual bosons exchanged in the process are the W^\pm bosons and the Higgs-ghosts Φ^\pm . The Yukawa coupling of the latter leads to an m_t^2/M_W^2 enhancement of the top quark contributions. Similarly a mass suppression follows from the Yukawa coupling to the charm quark which we consider as massless, $m_c^2/M_W^2 \approx 0$.

For the regularisation of ultraviolet and infrared divergences we use dimensional regularisation with $D = 4 - 2\varepsilon$ dimensions and work with the definition of an anticommuting γ_5 matrix $\{\gamma_\mu, \gamma_5\} = 0$ (NDR scheme). Furthermore, we employ the $\overline{\text{MS}}$ renormalisation scheme, i. e. we use the renormalization scale $\mu^2 e^{\gamma_E}/4\pi$ instead of μ^2 and subtract the poles in ε .

Since the construction of the eight-dimensional operator basis in (4) is based on the application of the equations of motions for the operators [19], only on-shell matrix elements are reproduced correctly [20] by the Hamiltonian (4). In the calculation of the diagrams we utilize the on-shell conditions $q^2 = (p_1 - p_2)^2 = 0$, $p_i^2 = m_i^2$ and apply the Dirac equation whenever possible. Here q^μ, p_1^μ, p_2^μ denote the momenta of the photon and the bottom and strange quarks respectively. The strange mass is neglected throughout ($m_s = 0$), except where it is needed for the regularisation of mass singularities.

A complete calculation of the vertex $\Gamma_{bs\gamma}^\mu$ in the full theory would take into account all possible 128 Feynman diagrams and the full dependence on all particle masses involved in these

diagrams. This is more information than is actually needed for the extraction of the Wilson coefficient $C_7(\mu_W)$. First of all, in the effective theory (4) terms of $\mathcal{O}(1/M^4)$ ($M = M_W, m_t$) are neglected by definition. For the matching procedure, the vertex $\Gamma_{bs\gamma}^\mu$ is correspondingly needed only up to $\mathcal{O}(1/M^2)$, i.e. up to the first nontrivial order of an expansion in the inverse heavy masses. Writing the most general structure of the vertex $\Gamma_{bs\gamma}^\mu$ in terms of some dimensionless structure functions \mathcal{F}_i

$$i\Gamma_{bs\gamma}^\mu = \frac{G_F}{\sqrt{2}}\lambda_t \frac{e}{4\pi^2} \bar{s}(p_2)(1 + \gamma_5) \left(\mathcal{F}_1 p_1^\mu m_b + \mathcal{F}_2 p_2^\mu m_b + \mathcal{F}_3 \gamma^\mu m_b^2 \right) b(p_1), \quad (22)$$

we then see that these structure functions are needed only at zeroth order in m_b/M_W , a fact that considerably simplifies the calculation. Secondly, even some information contained in (22) is redundant: from gauge invariance it follows that $q_\mu \Gamma_{bs\gamma}^\mu = 0$, implying

$$\mathcal{F}_3 = -\frac{\mathcal{F}_1 + \mathcal{F}_2}{2}. \quad (23)$$

Therefore the knowledge of \mathcal{F}_1 and \mathcal{F}_2 determines the vertex completely: all 40 diagrams contributing only to \mathcal{F}_3 can be neglected and are not listed in Figure 1. Using (23), one may finally write (22) as

$$i\Gamma_{bs\gamma}^\mu = -i\frac{G_F}{\sqrt{2}}\lambda_t \frac{e}{4\pi^2} K_7 \bar{s}(p_2) q_\nu \sigma^{\nu\mu} m_b (1 + \gamma_5) b(p_1) = -\frac{G_F}{\sqrt{2}}\lambda_t K_7 \langle Q_7 \rangle^{(0)} \quad (24)$$

with

$$K_7 = -\mathcal{F}_3 = \frac{\mathcal{F}_1 + \mathcal{F}_2}{2}. \quad (25)$$

This is the structure we already anticipated in (8)¹.

Finally, it should be stressed that our calculation was heavily supported by algebraic manipulation programs. We proceeded along two independent tracks, one based on FORM [21] and the other utilizing MATHEMATICA in combination with TRACER [22].

4.2 Heavy Mass Expansion

For calculating the vertex $\Gamma_{bs\gamma}^\mu$ up to $\mathcal{O}(m_b^2/M^2)$ we employed the so-called Heavy Mass Expansion which has developed into a widely used industry by now [23–26] (for a pedagogical description see also [27]). It approximates a Feynman integral $\langle \Gamma \rangle$ by the asymptotic expansion

$$\langle \Gamma \rangle \stackrel{M \rightarrow \infty}{\cong} \sum_{\gamma} C_{\gamma}^{(M)} \star \langle \Gamma/\gamma \rangle. \quad (26)$$

The notation of (26) is understood in the sense of the following prescription:

¹In deriving (24) we neglected the terms in (22) proportional to q^μ since they vanish after contraction with the polarization vector ϵ_μ ($\epsilon q = 0$).

- Identify all *hard subgraphs* γ of the diagram $\langle\Gamma\rangle$. A hard subgraph is defined as a 1PI part of the diagram that contains all lines with heavy masses M_W, m_t . The largest subgraph is the original diagram itself.
- Perform a formal Taylor series $C_\gamma^{(M)}$ in the integrand of these subgraphs with respect to its small quantities. Small quantities are small masses and the external momenta entering or leaving the subgraph. The Taylor expansion in particular includes the small bottom mass (the charm quark is considered as massless anyway), which cannot be neglected due to its explicit appearance in the operator Q_7 .
- Shrink the subgraph to an effective blob in the diagram and insert for it the Taylor expansion obtained in the previous step. Perform the integrations without any further expansions.
- Sum the contributions of all subgraphs.

The method is visualized for an example in Figure 3. The boxes indicate the Taylor expanded subgraphs $C_\gamma^{(M)}$ that are inserted in the blobs of the reduced diagrams $\langle\Gamma/\gamma\rangle$. Of the charm diagrams only those are non-vanishing which contain at least one W boson. This is due to the Yukawa suppression $m_c^2/M_W^2 = 0$ of the diagrams with Higgs-ghost exchange.

The Heavy Mass Expansion allows for an additional subdiagram in the charm contribution as compared to the top graph. This is the case where either the W propagator alone or the $WW\gamma$, $W\Phi\gamma$, $\Phi W\gamma$ vertices are identified as a subgraph γ_W which is not possible in a diagram with a virtual top quark, because the top mass is considered as heavy and has to be part of a subdiagram by definition. It turns out that it is not necessary to explicitly compute this contribution $\mathcal{M}_{\text{charm}}^{(\gamma_W)}$. This is for the following reason: due to the presence of two heavy propagators, the subgraphs $WW\gamma$, $W\Phi\gamma$, $\Phi W\gamma$ are of $\mathcal{O}(1/M^4)$, so they can be neglected for the matching with the effective theory which is accurate only to $\mathcal{O}(1/M^2)$. On the other hand, the subgraphs with the W propagator alone obviously yield the same contribution as the matrix element $\hat{\mathcal{M}}_2$ of the current-current operator Q_2 in the effective theory, so both contributions completely cancel each other in the matching procedure.

The contribution of the biggest, leading subgraph in the Heavy Mass Expansion — namely the one being the graph itself — just represents the naive expansion of the integrand in m_b/M . The virtues of the Heavy Mass Expansion are best seen by the way how the obvious deficits of this too simple approach are corrected by the contributions of the subleading subgraphs. First, the naive expansion alone results only in a polynomial power expansion of the parameter m_b/M , because by construction of the Taylor series the expansion parameter is nullified inside the integrals. Structures like logarithms $\ln(\mu^2/m_b^2)$ can only be generated from subleading subdiagram

contributions, where the bottom mass sets the integration scale in the reduced graph. Second, the expansion of the integrand in the leading subgraph may generate artificial infrared divergences. Similarly the expansion on the level of the subleading subgraph creates artificial divergences in the ultraviolet regime. These spurious divergences cancel each other in the sum of all subgraph contributions. The cancellation is only operative if ultraviolet and infrared poles are identified: $\varepsilon_{\text{UV}} = \varepsilon_{\text{IR}}$.

4.3 Classification of Integrals

From Figure 3 one can observe how the two-loop calculation is simplified by the Heavy Mass Expansion. The original massive two-loop integral with external momenta either reduces to a massive two-loop (tadpole) integral without external momenta or factorizes into two separate 1-loop integrals.

The diagrams of class 1 in Figure 1 with an internal top quark receive their contribution only from subdiagram γ_1 of the Heavy Mass Expansion, namely where γ_1 represents the graph itself. The master integral is a two-loop tadpole integral with one massless and two massive lines of different mass [28]

$$\begin{aligned} \mu^{4\varepsilon} \int \frac{d^D p}{(2\pi)^D} \int \frac{d^D k}{(2\pi)^D} \frac{1}{(m_t^2 - p^2)(M_W^2 - k^2)(-[p+k]^2)} = \\ \left(\frac{4\pi\mu^2}{M_W^2} e^{-\gamma_E} \right)^{2\varepsilon} \left(\frac{i}{16\pi^2} \right)^2 M_W^2 \left\{ \begin{aligned} & -\frac{1}{\varepsilon^2} \frac{1}{2} (1+x_t) + \frac{1}{\varepsilon} \left[-\frac{3}{2} (1+x_t) + x_t \ln x_t \right] \\ & + (1+x_t) \left[-\frac{7}{2} - \frac{\pi^2}{12} \right] - (1-x_t) \text{Li}_2(1-x_t) \\ & + 3x_t \ln x_t - \frac{1}{2} x_t \ln^2 x_t \end{aligned} \right\} \end{aligned} \quad (27)$$

where $\text{Li}_2(x) = -\int_0^x dt \frac{\ln(1-t)}{t}$. Due to the expansion, integrals occur also with higher powers in the denominator. They are easily obtained from (27) by taking derivatives with respect to the masses. Higher powers in the massless propagator require a separate calculation. As an example we give the result for the integral with a quadratic massless propagator:

$$\begin{aligned} \mu^{4\varepsilon} \int \frac{d^D p}{(2\pi)^D} \int \frac{d^D k}{(2\pi)^D} \frac{1}{(m_t^2 - p^2)(M_W^2 - k^2)(-[p+k]^2)^2} = \\ \left(\frac{4\pi\mu^2}{M_W^2} e^{-\gamma_E} \right)^{2\varepsilon} \left(\frac{i}{16\pi^2} \right)^2 \left\{ \begin{aligned} & -\frac{1}{2\varepsilon^2} + \frac{1}{\varepsilon} \left[-\frac{1}{2} + \frac{x_t}{x_t-1} \ln x_t \right] \\ & -\frac{1}{2} - \frac{\pi^2}{12} + \frac{x_t+1}{x_t-1} \text{Li}_2(1-x_t) \\ & + \frac{x_t}{x_t-1} \ln x_t - \frac{x_t}{2(x_t-1)} \ln^2 x_t \end{aligned} \right\}. \end{aligned} \quad (28)$$

Massless lines are raised at most to a power of 4 in the expansion. The corresponding integrals are computed in an analogous manner.

For all four classes of diagrams the subgraph γ_1 contributions can be reduced by partial fractioning to the above integrals and to the special case of two equal masses

$$\begin{aligned} \mu^{4\epsilon} \int \frac{d^D p}{(2\pi)^D} \int \frac{d^D k}{(2\pi)^D} \frac{1}{(M^2 - p^2)^\alpha (M^2 - k^2)^\beta (-[p+k]^2)^\gamma} = \\ \left(\frac{4\pi\mu^2}{M^2}\right)^{2\epsilon} \left(\frac{i}{16\pi^2}\right)^2 (M^2)^{4-\alpha-\beta-\gamma} \\ \frac{\Gamma(\alpha + \beta + \gamma - D)\Gamma(\alpha + \gamma - D/2)\Gamma(\beta + \gamma - D/2)\Gamma(D/2 - \gamma)}{\Gamma(\alpha)\Gamma(\beta)\Gamma(D/2)\Gamma(\alpha + \beta + 2\gamma - D)}. \end{aligned} \quad (29)$$

In case of an internal charm quark only one heavy mass M_W is present in the subgraphs γ_1 . The corresponding tadpole integral reads

$$\begin{aligned} \mu^{4\epsilon} \int \frac{d^D p}{(2\pi)^D} \int \frac{d^D k}{(2\pi)^D} \frac{1}{(M^2 - p^2)^\alpha (-k^2)^\beta (-[p+k]^2)^\gamma} = \\ \left(\frac{4\pi\mu^2}{M^2}\right)^{2\epsilon} \left(\frac{i}{16\pi^2}\right)^2 (M^2)^{4-\alpha-\beta-\gamma} \\ \frac{\Gamma(D/2 - \gamma)\Gamma(D/2 - \beta)\Gamma(\beta + \gamma - D/2)\Gamma(\alpha + \beta + \gamma - D)}{\Gamma(\alpha)\Gamma(\beta)\Gamma(\gamma)\Gamma(D/2)}. \end{aligned} \quad (30)$$

Different types of integrals come into play during the calculation of the contributions from the second subgraphs γ_2 . Whereas the subdiagrams themselves amount to a trivial one-loop tadpole integral, the reduced graphs $\langle \Gamma/\gamma_2 \rangle$ lead to many different kinds of massive one-loop integrals with nonvanishing external momenta. They are computed in the standard manner.

As far as the reduced graphs are concerned, class 2 diagrams are characterized by two-point functions with the quark being either the bottom or the strange quark. Some of the integrals containing the strange quark become singular in the small m_s limit. In these cases the strange mass has to be kept as a regulator, but can be neglected otherwise.

In classes 3 and 4 three-point functions must be calculated with either two different or two equal masses. In the presence of a strange quark again its mass m_s serves as a regulator for mass singularities.

4.4 Results

The matrix element calculated in the full theory,

$$\mathcal{M}(b \rightarrow s\gamma) = \mathcal{M}_{\text{top}}(b \rightarrow s\gamma) + \mathcal{M}_{\text{charm}}(b \rightarrow s\gamma), \quad (31)$$

receives contributions from diagrams with a virtual top and a virtual charm quark respectively. Because the formula for the top contribution is rather lengthy we do not reproduce it here, but give — as a separate intermediate result — the charm part of the two-loop matrix element alone ($r = m_s^2/m_b^2$):

$$\begin{aligned} \mathcal{M}_{\text{charm}}^{(1)} &= -\frac{G_F}{\sqrt{2}} \lambda_t \langle s\gamma|Q_7|b\rangle^{(0)} \frac{\alpha_s}{4\pi} \\ &\cdot \left(-\frac{1}{972}\right) \left\{ \frac{210}{\varepsilon} - \frac{828}{\varepsilon} \ln r \left[1 + \varepsilon \ln \frac{\mu^2}{m_b^2} + \varepsilon \ln \frac{\mu^2}{M_W^2} \right] \right. \\ &\quad \left. - 3155 - 96\pi^2 + 288i\pi - 2526 \ln r + 414 \ln^2 r - 1134 \ln \frac{\mu^2}{m_b^2} + 1554 \ln \frac{\mu^2}{M_W^2} \right\} \\ &+ \mathcal{M}_{\text{charm}}^{(\gamma W)}. \end{aligned} \quad (32)$$

As discussed before, the subgraph piece $\mathcal{M}_{\text{charm}}^{(\gamma W)}$ of the Heavy Mass Expansion will cancel in the matching and needs not to be calculated explicitly.

The complete (unrenormalized) two-loop result is obtained after adding the top quark contribution to (32). We express it with the help of two auxiliary functions

$$g_t = -6x_t \frac{\partial C_{70}^{(0)}}{\partial x_t}, \quad (33)$$

$$g_b = \frac{x_t(3x_t - 4)}{4(x_t - 1)^3} \ln x_t + \frac{x_t(9 - 7x_t)}{8(x_t - 1)^2}. \quad (34)$$

One arrives at

$$\mathcal{M}^{(1)}(b \rightarrow s\gamma) = -\frac{G_F}{\sqrt{2}} \lambda_t \frac{\alpha_s}{4\pi} \Delta_{\text{full}}^{\text{unren}} + \mathcal{M}_{\text{charm}}^{(\gamma W)} \quad (35)$$

where

$$\Delta_{\text{full}}^{\text{unren}} = C_7^{(0)}(\mu_W) \langle Q_7 \rangle^{(1)} + \frac{4}{3} \langle Q_7 \rangle^{(0)} \left[g_1 \frac{1}{\varepsilon} \left(\frac{\mu^2}{M_W^2} \right)^{2\varepsilon} + g_2 \frac{1}{2} \ln \frac{m_b^2}{M_W^2} + g_3 \right] \quad (36)$$

with

$$g_1 = -g_b - g_t + C_{70}^{(0)} + \frac{23}{27}, \quad (37)$$

$$g_2 = 2 \left(g_b + 3C_{70}^{(0)} - \frac{4}{3}C_{80}^{(0)} \right) + \frac{4}{9}, \quad (38)$$

$$\begin{aligned} g_3 &= \frac{x_t(4 - 40x_t + 61x_t^2 + 8x_t^3)}{6(x_t - 1)^4} \text{Li}_2(1 - x_t) + \frac{2}{3}i\pi C_{80}^{(0)} - \frac{2}{9}\pi^2 C_{80}^{(0)} \\ &+ \frac{x_t(-20 - 125x_t + 149x_t^2 + 196x_t^3 + 16x_t^4)}{24(x_t - 1)^5} \ln x_t^2 \\ &+ \frac{416 - 3448x_t + 9431x_t^2 - 6273x_t^3 - 2826x_t^4 - 540x_t^5}{216(x_t - 1)^5} \ln x_t \\ &+ \frac{-872 + 4352x_t - 33369x_t^2 + 44732x_t^3 + 4597x_t^4}{1296(x_t - 1)^4}. \end{aligned} \quad (39)$$

The leading order coefficients were already given in (16), (17) and (18). In (36) we have separated the term $C_7^{(0)}\langle Q_7 \rangle^{(1)}$ which — as can be seen in (14) — will be cancelled precisely in the process of matching by the corresponding term in the effective theory. For completeness the explicit expression of $\langle Q_7 \rangle^{(1)}$ is given in (54). Inserting it into (35) one recovers the corresponding formula in [7].

4.5 Renormalization

We will now give the counterterms necessary to renormalize the full theory in the \overline{MS} scheme.

4.5.1 Top Quark Mass Renormalization

The simplest method to find the counterterm related to the top quark mass renormalization is to take the result for $C_7^{(0)}$ in (15) (including the ε terms) and replace there m_t as follows

$$m_t \rightarrow m_t + (Z_{m_t} - 1)m_t \quad (40)$$

where

$$Z_{m_t} = 1 - \frac{\alpha_s}{4\pi} \frac{4}{\varepsilon}. \quad (41)$$

Expanding then in α_s , extracting the coefficient of $\alpha_s/(4\pi)$ and multiplying it by $\langle Q_7 \rangle^{(0)}$ gives the counterterm to be added to $\Delta_{\text{full}}^{\text{unren}}$ in (35):

$$\Delta_{m_t}^c = \frac{4}{3} \left[\frac{1}{\varepsilon} g_t - 6x_t \frac{\partial C_{7\varepsilon}^{(0)}(\mu_W)}{\partial x_t} \right] \langle Q_7 \rangle^{(0)}. \quad (42)$$

Another method is to perform the top mass renormalization diagram by diagram by considering separately the renormalization of m_t in the top quark propagator as well as in its Yukawa coupling to the Higgs-ghosts Φ^\pm . This much more involved method has been used in the two-loop calculations of QCD corrections to the Z^0 -penguin in [29]. We have checked that this method also gives the result in (42). $\Delta_{m_t}^c$ in (42) reproduces the corresponding counterterm in [7].

4.5.2 Bottom Quark Mass Renormalization

The bottom masses entering the amplitude are of twofold origin. Those b quark masses that are introduced via the Dirac-equation or the on-shell condition $p_1^2 = m_b^2$ represent the renormalized on-shell quark mass and are not subject to the mass renormalization. Consequently, the m_b renormalization refers only to m_b entering the b quark Yukawa couplings to the Higgs-ghosts

Φ^\pm . Since we work with on-shell b quarks in our calculations we must use the on-shell mass renormalization function

$$Z_{m_b} = 1 - \frac{\alpha_s}{4\pi} \left(\frac{4}{\varepsilon} + 4 \ln \frac{\mu^2}{m_b^2} + \frac{16}{3} \right). \quad (43)$$

We therefore replace m_b in the Yukawa couplings in the one-loop diagrams contributing to $C_7^{(0)}(\mu_W)$ as follows

$$m_b \rightarrow m_b + (Z_{m_b} - 1)m_b. \quad (44)$$

The coefficient of $\alpha_s/(4\pi)$ then gives the m_b counterterm to be added to $\Delta_{\text{full}}^{\text{unren}}$ in (35):

$$\Delta_{m_b}^c = \frac{4}{3} \left[g_b(x_t) \left(\frac{2}{\varepsilon} + 2 \ln \frac{\mu^2}{m_b^2} + \frac{8}{3} \right) + \bar{g}_b(x_t) \right] \left(\frac{\mu^2}{M_W^2} \right)^\varepsilon \langle Q_7 \rangle^{(0)}. \quad (45)$$

Here $g_b(x_t)$ is defined in (34) and $\bar{g}_b(x_t)$ is given by

$$\bar{g}_b(x_t) = \frac{4x_t - 3x_t^2}{8(x_t - 1)^3} \ln^2 x_t + \frac{10x_t^3 - 13x_t^2}{8(x_t - 1)^3} \ln x_t + \frac{25x_t - 19x_t^2}{16(x_t - 1)^2}. \quad (46)$$

$\Delta_{m_b}^c$ in (45) agrees with the corresponding result in [7].

4.5.3 External Leg Wave Function Renormalization

This renormalization can be avoided as it has to cancel with the corresponding renormalization in the effective theory: this feature is not respected in the calculation of [7] as δR_Z in their equation (3.13) does not equal to $\delta \hat{R}_Z$ in (4.15) in the effective theory. By reintroducing $\mathcal{O}(\varepsilon)$ terms in $C_7^{(0)}$ in $\delta \hat{R}_Z$ one recovers $\delta R_Z = \delta \hat{R}_Z$ as it should be.

4.6 Summary of the Result in the Full Theory

Dropping $\mathcal{M}_{\text{charm}}^{(\gamma W)}$ and the contribution of the wave function renormalization of the external quarks that will be cancelled by corresponding terms in the effective theory we find the right hand side of the matching relation (14):

$$K_7^{(1)} \langle Q_7 \rangle^{(0)} = \Delta_{\text{full}}^{\text{unren}} + \Delta_{m_t}^c + \Delta_{m_b}^c, \quad (47)$$

where $\Delta_{\text{full}}^{\text{unren}}$, $\Delta_{m_t}^c$ and $\Delta_{m_b}^c$ are given in (36), (42), and (45), respectively.

5 Calculation of $b \rightarrow s\gamma$ in the Effective Theory

5.1 Unrenormalized Contributions

In order to perform the NLO matching and extract $C_7^{(1)}$ from the matching relation (14), the knowledge of all other quantities in (14) is required.

Due to the identity of the matrix element $\hat{\mathcal{M}}_2$ of the operator Q_2 in the effective theory with the charm contribution $\mathcal{M}_{\text{charm}}^{(\gamma W)}$ in the full theory,

$$\hat{\mathcal{M}}_2(b \rightarrow s\gamma) = \mathcal{M}_{\text{charm}}^{(\gamma W)}(b \rightarrow s\gamma), \quad (48)$$

both contributions drop out from the left and the right hand side of (14). In what follows we will discuss the remaining contributions in the effective theory.

Since the Wilson coefficients for the operators $Q_1, Q_3 \dots, Q_6$ start at order α_s^1 only their LO (α_s^0) one-loop matrix elements $\langle s\gamma|Q_i|b\rangle^{(0)}$ are of relevance. Additionally it was shown in [30] that only the one-loop matrix elements of Q_5 and Q_6 do not vanish in the NDR scheme. Their contribution to $\hat{\mathcal{M}}(b \rightarrow s\gamma)$ is

$$\hat{\mathcal{M}}_{5+6} = -\frac{G_F}{\sqrt{2}} \lambda_t \left[C_5(\mu_W) \langle Q_5 \rangle^{(0)} + C_6(\mu_W) \langle Q_6 \rangle^{(0)} \right] \quad (49)$$

where

$$\langle Q_5 \rangle^{(0)} = -\frac{1}{3} \langle Q_7 \rangle^{(0)} \left(\frac{\mu^2}{m_b^2} \right)^\varepsilon, \quad \langle Q_6 \rangle^{(0)} = -\langle Q_7 \rangle^{(0)} \left(\frac{\mu^2}{m_b^2} \right)^\varepsilon, \quad (50)$$

and the coefficient functions C_5, C_6 are given by [10]

$$C_5(\mu) = \frac{\alpha_s(\mu)}{4\pi} \left[-\frac{1}{9} \ln \frac{\mu^2}{M_W^2} - \frac{1}{6} \tilde{E}(x_t) \right], \quad C_6(\mu) = \frac{\alpha_s(\mu)}{4\pi} \left[\frac{1}{3} \ln \frac{\mu^2}{M_W^2} + \frac{1}{2} \tilde{E}(x_t) \right] \quad (51)$$

with

$$\tilde{E}(x_t) = -\frac{2}{3} \ln x_t + \frac{x_t^2(15 - 16x_t + 4x_t^2)}{6(1 - x_t)^4} \ln x_t + \frac{x_t(18 - 11x_t - x_t^2)}{12(1 - x_t)^3} - \frac{2}{3}. \quad (52)$$

Since the matrix elements of Q_5 and Q_6 are finite, the possible $\mathcal{O}(\varepsilon)$ terms in C_5 and C_6 can be set to zero. Similarly the $\mathcal{O}(\varepsilon)$ terms in (50) can be omitted. We will need them, however, in Section 5.2.2 in the process of renormalization in the effective theory. Removing the overall factor in (49) and $\alpha_s/(4\pi)$ we obtain the contribution of the operators Q_5 and Q_6 to the left hand side of the matching condition in (14):

$$\hat{\Delta}_{5+6} = -\frac{4}{9} \left(\frac{2}{3} \ln \frac{\mu^2}{M_W^2} + \tilde{E}(x_t) \right) \langle Q_7 \rangle^{(0)}. \quad (53)$$

The matrix element of the operator Q_8 is zero at tree level, thus making the knowledge of $C_8^{(1)}$ superfluous for the matching.

One remains left with the one-loop matrix elements of the operators Q_7 and Q_8 . They are calculated in the effective theory where the diagrams in Figure 2 have to be considered. The circles indicate the insertions of the operators. The computation of the corresponding

massive three-point function leads to the following results for the (unrenormalized) one-loop matrix elements [14, 15]

$$\langle Q_7 \rangle^{(1)} = \frac{4}{3} \left[-\frac{1}{\varepsilon} \ln r + \frac{1}{2} \ln^2 r - \ln r \ln \frac{\mu^2}{m_b^2} - 2 \ln r \right] \langle Q_7 \rangle^{(0)}, \quad (54)$$

$$\langle Q_8 \rangle^{(1)} = \left(-\frac{4}{27} \right) \left[-\frac{12}{\varepsilon} - 33 + 2\pi^2 - 12 \ln \frac{\mu^2}{m_b^2} - 6i\pi \right] \langle Q_7 \rangle^{(0)}. \quad (55)$$

Again the strange quark mass acts as an infrared regulator in $r = (m_s^2/m_b^2)$. In summary the left hand side of the matching condition in (14) prior to the renormalization is given as follows

$$\Delta_{\text{eff}}^{\text{unren}} = \hat{\Delta}_{5+6} + C_7^{(0)}(\mu_W) \langle Q_7 \rangle^{(1)} + C_8^{(0)}(\mu_W) \langle Q_8 \rangle^{(1)} + C_7^{(1)}(\mu_W) \langle Q_7 \rangle^{(0)} \quad (56)$$

where $C_7^{(1)}(\mu_W)$ is the coefficient we are looking for. Since the matrix elements (54), (55) contain divergences, it is necessary to keep the $\mathcal{O}(\varepsilon)$ terms in $C_7^{(0)}$ and $C_8^{(0)}$ in (56).

5.2 Renormalization

5.2.1 Bottom Quark Mass Renormalization

In the effective theory the amplitude receives a contribution from the term

$$C_7^{(0)}(\mu_W) \langle s\gamma | Q_7 | b \rangle^{(0)} \quad (57)$$

where, as seen in (5), Q_7 is linear in m_b . Making the replacement (44) in Q_7 one generates a counterterm to be added to the left hand side of the matching condition (14):

$$\hat{\Delta}_{m_b}^c = - \left(\frac{4}{\varepsilon} + 4 \ln \frac{\mu^2}{m_b^2} + \frac{16}{3} \right) C_7^{(0)}(\mu_W) \langle Q_7 \rangle^{(0)}. \quad (58)$$

This result agrees with the corresponding result in [7] except for the $\mathcal{O}(\varepsilon)$ terms in $C_7^{(0)}(\mu_W)$ which have been omitted by these authors.

5.2.2 Operator Renormalization

The renormalization of the operator matrix elements involves the operator renormalization and the wave function renormalization of the quark fields. We do not include the latter as this renormalization cancels in the process of matching with the corresponding renormalization in the full theory. We have discussed this issue in Section 4.5.3.

Since the operator renormalization is $\mathcal{O}(\alpha_s)$, only the counterterms for the matrix elements of the operators Q_2 , Q_7 and Q_8 have to be considered. These counterterms can easily be calculated

by using the leading order operator renormalization constants [30] or directly by using the relevant coefficients of $\alpha_s/(4\pi)$ in the leading anomalous dimension matrix $\hat{\gamma}^{(0)}$.

For the operators Q_7 and Q_8 the counterterms contributing to the left hand side of the matching condition (14) are simply given by

$$\hat{\Delta}_{77}^c = \frac{1}{\varepsilon} \frac{\gamma_{77}^{(0)}}{2} C_7^{(0)} \langle Q_7 \rangle^{(0)}, \quad \hat{\Delta}_{87}^c = \frac{1}{\varepsilon} \frac{\gamma_{87}^{(0)}}{2} C_8^{(0)} \langle Q_7 \rangle^{(0)} \quad (59)$$

where $\gamma_{77}^{(0)} = 32/3$ and $\gamma_{87}^{(0)} = -32/9$. The corresponding counterterms for Q_2 , related to its mixing under renormalization with the operators Q_5 and Q_6 , are given by (with $C_2^{(0)} = 1$)

$$\hat{\Delta}_{25}^c = \frac{1}{\varepsilon} \frac{\gamma_{25}^{(0)}}{2} \langle Q_5 \rangle^{(0)}, \quad \hat{\Delta}_{26}^c = \frac{1}{\varepsilon} \frac{\gamma_{26}^{(0)}}{2} \langle Q_6 \rangle^{(0)} \quad (60)$$

with $\langle Q_5 \rangle^{(0)}$ and $\langle Q_6 \rangle^{(0)}$ given in (50) and $\gamma_{25}^{(0)} = -2/9$, $\gamma_{26}^{(0)} = 2/3$.

The leading anomalous dimension $\gamma_{27}^{(0)}$ related to the mixing of the operators Q_2 and Q_7 is obtained from two-loop calculations as opposed to (59) and (60) which involve one-loop calculations. Because this time the mixing of operators with different dimensions (in $D \neq 4$ dimensions of space-time) is considered, the relation between the relevant operator renormalization constant and $\gamma_{27}^{(0)}$ is more involved [19]. One finds:

$$\hat{\Delta}_{27}^c = \frac{1}{\varepsilon} \frac{\gamma_{27}^{(0)\text{NDR}}}{4} \langle Q_7 \rangle^{(0)} \quad (61)$$

with $\gamma_{27}^{(0)\text{NDR}} = 464/81$.

5.3 Summary of the Result in the Effective Theory

Adding the counterterms (58), (59), (60) and (61) to the unrenormalized result in (56) we obtain the final result for the left hand side of the matching condition (14)

$$\sum_{i=1}^8 \left(C_i^{(0)} \langle Q_i \rangle^{(1)} + C_i^{(1)} \langle Q_i \rangle^{(0)} \right) = \Delta_{\text{eff}}^{\text{unren}} + \hat{\Delta}_{m_b}^c + \hat{\Delta}_{77}^c + \hat{\Delta}_{87}^c + \hat{\Delta}_{25}^c + \hat{\Delta}_{26}^c + \hat{\Delta}_{27}^c. \quad (62)$$

6 Result for the Initial Condition $C_7(\mu_W)$

The initial condition $C_7^{(1)}(\mu_W)$ can now be determined from the NLO matching relation (14) by inserting (47) and (62) and solving for the unknown $C_7^{(1)}(\mu_W)$. One arrives at the final result

$$C_7^{(1)}(\mu_W) = C_7^{(1)}(M_W) + 8x_t \frac{\partial C_7^{(0)}(\mu_W)}{\partial x_t} \ln \frac{\mu_t^2}{M_W^2} + \left(\frac{16}{3} C_7^{(0)}(\mu_W) - \frac{16}{9} C_8^{(0)}(\mu_W) + \frac{\gamma_{27}^{(0)\text{NDR}}}{2} \right) \ln \frac{\mu_W^2}{M_W^2} \quad (63)$$

where

$$\begin{aligned}
C_7^{(1)}(M_W) &= \frac{2x_t(4 - 40x_t + 61x_t^2 + 8x_t^3)}{9(x_t - 1)^4} \text{Li}_2(1 - x_t) \\
&+ \frac{x_t(-4 - 40x_t + 37x_t^2 + 71x_t^3 + 8x_t^4)}{9(x_t - 1)^5} \ln^2 x_t \\
&+ \frac{2(116 - 742x_t + 1697x_t^2 - 1158x_t^3 - 294x_t^4 - 51x_t^5)}{81(x_t - 1)^5} \ln x_t \\
&+ \frac{-580 + 3409x_t - 12126x_t^2 + 12961x_t^3 + 1520x_t^4}{486(x_t - 1)^4}
\end{aligned} \tag{64}$$

and $\gamma_{27}^{(0)\text{NDR}} = 464/81$. Thus we confirm the findings of [6] and [7]. Our formula generalizes the results of these papers in the sense that we distinguish between the scale dependence of the matching scale μ_W and the dependence on the mass scale μ_t at which the running top quark mass $\overline{m}_t(\mu_t)$ is defined. Both scales are not necessarily equal, but were identified $\mu_W = \mu_t = \mu_{Wt}$ in [6, 7]. In [17] the separate cancellation of these scales dependent terms in the sum of the LO and NLO contribution is demonstrated and the phenomenological implications are discussed.

For completion we also quote the results for the contribution of the magnetic gluon-penguin operator as calculated in [6, 7] and generalized to $\mu_W \neq \mu_t$ in [17]

$$C_8^{(1)}(\mu_W) = C_8^{(1)}(M_W) + 8x_t \frac{\partial C_8^{(0)}(\mu_W)}{\partial x_t} \ln \frac{\mu_t^2}{M_W^2} + \left(\frac{14}{3} C_8^{(0)}(\mu_W) + \frac{\gamma_{28}^{(0)\text{NDR}}}{2} \right) \ln \frac{\mu_W^2}{M_W^2} \tag{65}$$

with

$$\begin{aligned}
C_8^{(1)}(M_W) &= \frac{x_t(-1 - 41x_t - 40x_t^2 + 4x_t^3)}{6(x_t - 1)^4} \text{Li}_2(1 - x_t) \\
&+ \frac{x_t(1 - 146x_t - 103x_t^2 - 44x_t^3 + 4x_t^4)}{12(x_t - 1)^5} \ln^2 x_t \\
&+ \frac{304 - 2114x_t + 3007x_t^2 + 4839x_t^3 + 1086x_t^4 - 210x_t^5}{216(x_t - 1)^5} \ln x_t \\
&+ \frac{-652 + 1510x_t - 29595x_t^2 - 13346x_t^3 + 611x_t^4}{1296(x_t - 1)^4}
\end{aligned} \tag{66}$$

and $\gamma_{28}^{(0)\text{NDR}} = 76/27$.

In the phenomenological applications it is more convenient to work with the effective coefficients [5]

$$C_7^{\text{eff}}(\mu_W) = C_7(\mu_W) - \frac{1}{3} C_5(\mu_W) - C_6(\mu_W) \tag{67}$$

and

$$C_8^{\text{eff}}(\mu_W) = C_8(\mu_W) + C_5(\mu_W). \tag{68}$$

Using (51), (63) and (65) one finds the effective coefficients used in [17]. For $\mu_t = \mu_W = M_W$ these effective coefficients reduce to the ones given in [13].

7 Summary

In this paper we have calculated the initial condition for the Wilson coefficient of the magnetic photon-penguin operator at next-to-leading order. Our result agrees with the ones presented in [6, 7]. The method used by us is very different from the one of Adel and Yao [6], but is rather similar to the one of Greub and Hurth [7]. However, in contrast to the latter authors, we are able to obtain the final result by calculating only the virtual corrections to $b \rightarrow s\gamma$ without invoking the gluon bremsstrahlung $b \rightarrow s\gamma g$ as done in [7]. To this end it was necessary to keep in the process of matching $\mathcal{O}(\varepsilon)$ terms in the leading order Wilson coefficients. Our main result, which generalizes the results of [6, 7] to $\mu_W \neq \mu_t$, is given in (63). The numerical analysis of these formulae in the context of a complete NLO analysis of the decay $B \rightarrow X_s\gamma$ has been presented in [17].

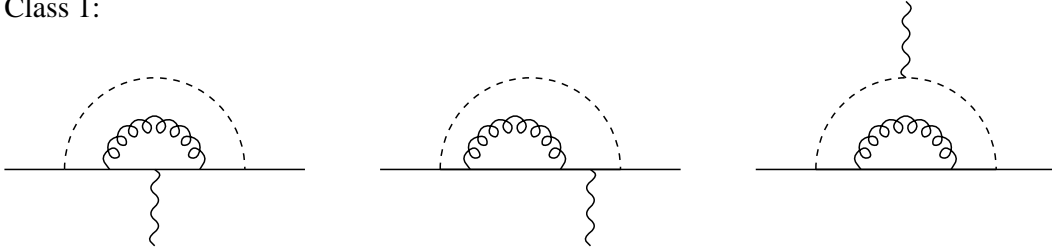
References

- [1] S. BERTOLINI, F. BORZUMATI AND A. MASIERO, *Phys. Rev. Lett.* **59** (1987) 180; N.G. DESHPANDE, P. LO, J. TRAMPETIC, G. EILAM AND P. SINGER, *Phys. Rev. Lett.* **59** (1987) 183.
- [2] M.S. ALAM *et al.* (CLEO collaboration), *Phys. Rev. Lett.* **74** (1995) 2885.
- [3] ALEPH COLLABORATION, result quoted by P. DRELL at the XVIII *International Symposium on Lepton-Photon Interactions, Hamburg 1997*.
- [4] A. ALI AND C. GREUB, *Z. Phys.* **C60** (1993) 433.
- [5] A. J. BURAS, M. MISIAK, M. MÜNZ AND S. POKORSKI, *Nucl. Phys.* **B424** (1994) 374.
- [6] K. ADEL AND Y. P. YAO, *Phys. Rev.* **D49** (1994) 4945.
- [7] C. GREUB AND T. HURTH, *Phys. Rev.* **D56** (1997) 2934.
- [8] G. ALTARELLI, G. CURCI, G. MARTINELLI AND S. PETRARCA, *Nucl. Phys.* **B187** (1981) 461.
- [9] A. J. BURAS AND P. H. WEISZ, *Nucl. Phys.* **B333** (1990) 66.
- [10] A. J. BURAS, M. JAMIN, M. E. LAUTENBACHER AND P. H. WEISZ, *Nucl. Phys.* **B370** (1992) 69; *Nucl. Phys.* **B375** (1992) 501 (addendum); *Nucl. Phys.* **B400** (1993) 37.

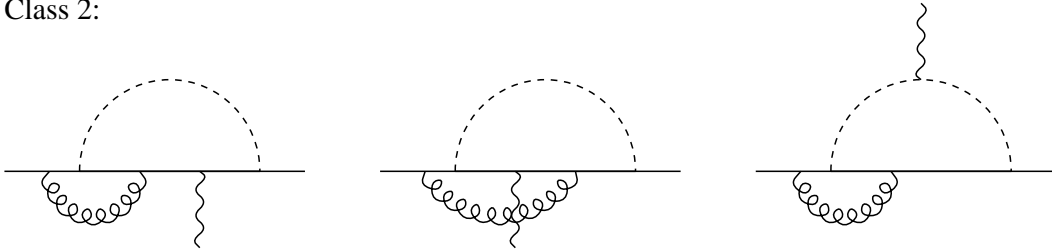
- [11] M. CIUCHINI, E. FRANCO, G. MARTINELLI AND L. REINA, *Phys. Lett.* **B301** (1993) 263; *Nucl. Phys.* **B415** (1994) 403.
- [12] M. MISIAK AND M. MÜNZ, *Phys. Lett.* **B344** (1995) 308.
- [13] K.G. CHETYRKIN, M. MISIAK AND M. MÜNZ, *Phys. Lett.* **B400** (1997) 206;
- [14] A. ALI AND C. GREUB, *Z. Phys.* **C49** (1991) 431; *Phys. Lett.* **B361** (1995) 146.
- [15] N. POTT, *Phys. Rev.* **D54** (1996) 938.
- [16] C. GREUB, T. HURTH AND D. WYLER, *Phys. Lett.* **B380** (1996) 385; *Phys. Rev.* **D54** (1996) 3350;
- [17] A.J. BURAS, A. KWIATKOWSKI AND N. POTT, *preprint* TUM-HEP-287/97 [hep-ph/9707482], to appear in *Phys. Lett. B*.
- [18] G. BUCHALLA, A.J. BURAS AND M. LAUTENBACHER, *Rev. Mod. Phys.* **68** (1996) 1125.
- [19] B. GRINSTEIN, R. SPRINGER AND M. B. WISE, *Nucl. Phys.* **B339** (1990) 269.
- [20] H.D. POLITZER, *Nucl. Phys.* **B172** (1980) 349;
H. SIMMA, *Z. Phys. C* **61** (1994) 67.
- [21] J.A.M. VERMASEREN, *Symbolic Manipulation with FORM, Version 2*, CAN, Amsterdam 1991.
- [22] M. JAMIN AND M.E. LAUTENBACHER, *Comp. Phys. Commun.* **74** (1993) 265.
- [23] G.B. PIVOVAROV AND F.V. TKACHOV, *preprint* INR P-0379 (1984);
F.V. TKACHOV, *Int. J. Mod. Phys.* **A8** (1993) 2047;
G.B. PIVOVAROV AND F.V. TKACHOV, *Int. J. Mod. Phys.* **A8** (1993) 2241.
- [24] S.G. GORISHNY AND S.A. LARIN, *Nucl. Phys.* **B287** (1987) 452;
S.G. GORISHNY, *Nucl. Phys.* **B319** (1989) 633.
- [25] K.G. CHETYRKIN AND V.A. SMIRNOV *preprint* INR P-518 (1987);
K.G. CHETYRKIN, *preprint* MPI-PAE/PTH 13/91 (1991);
V.A. SMIRNOV, *Commun. Math. Phys.* **134** (1990) 109.
- [26] V.A. SMIRNOV, *Renormalization and Asymptotic Expansions*, Birkhäuser, Basel 1991.
- [27] K.G. CHETYRKIN, J.H. KÜHN AND A. KWIATKOWSKI, *Phys. Rept.* **277** (1996) 189.

- [28] J.J. VAN DER BIJ AND M. VELTMAN, *Nucl. Phys.* **B248** (1984) 141;
J.J. VAN DER BIJ AND A. GHINCULOV, *Nucl. Phys.* **B436** (1995) 30.
- [29] G. BUCHALLA AND A. J. BURAS, *Nucl. Phys.* **B398** (1993) 285.
- [30] M. CIUCHINI, E. FRANCO, G. MARTINELLI, L. REINA AND L. SILVESTRINI, *Phys. Lett.* **B316** (1993) 127, *Nucl. Phys.* **B421** (1994) 41; M. MISIAK *Nucl. Phys.* **B393** (1993) 23, *Nucl. Phys.* **B439** (1995) 461; G. CELLA, G. CURCI, G. RICCIARDI AND A. VICERÉ, *Phys. Lett.* **B325** (1994) 227; *Nucl. Phys.* **B431** (1994) 417.

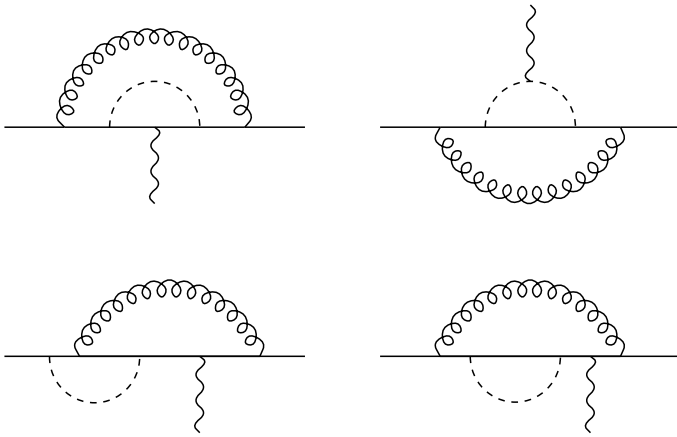
Class 1:



Class 2:



Class 3:



Class 4:

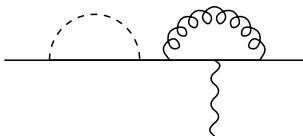


Figure 1: The Feynman graphs contributing to $b \rightarrow s\gamma$ in the full theory. The internal quark is either a top or a charm, and every dashed line can be a W^\pm boson or a Higgs-ghost Φ^\pm . Left-right symmetric diagrams and diagrams contributing only to the structure function \mathcal{F}_3 (see text) are not shown.

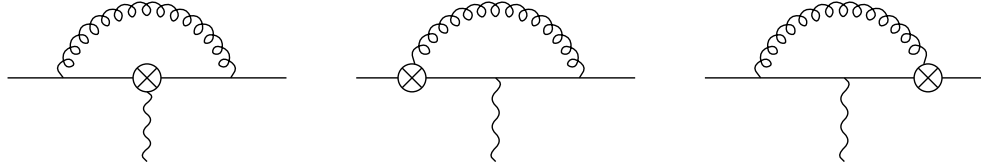


Figure 2: The three $b \rightarrow s\gamma$ Feynman graphs of the effective theory involving the operators Q_7 and Q_8 . Four additional diagrams containing Q_8 are not shown since they contribute only to the structure function \mathcal{F}_3 (see text).

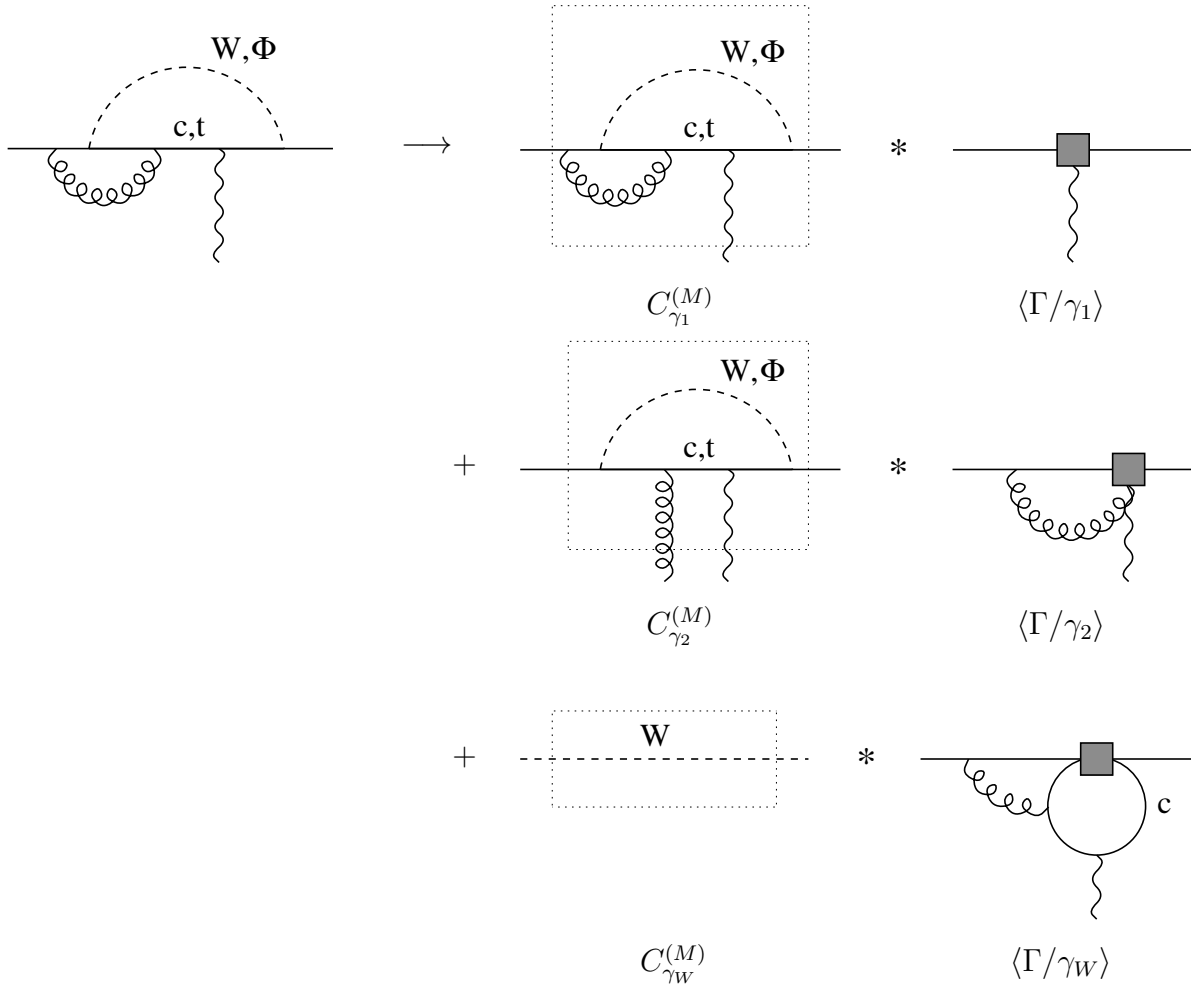


Figure 3: Pictorial representation of the Heavy Mass Expansion. The third term only exists if the internal quark is a charm.